

# New Insights on Land Surface-Atmosphere Feedbacks over Tropical South America at Interannual Timescales

Juan Mauricio Bedoya-Soto <sup>1,\*</sup>, Germán Poveda <sup>1</sup> and David Sauchyn <sup>2</sup>

<sup>1</sup> Departamento de Geociencias y Ambiente, Facultad de Minas, Universidad Nacional de Colombia, Sede Medellín, Medellín, 050041, Colombia; gpoveda@unal.edu.co

<sup>2</sup> Department of Geography and Environmental Studies, University of Regina, Regina, SK, S4S0A2, Canada; David.Sauchyn@uregina.ca

\* Correspondence: jmbedoya@unal.edu.co; Tel.: 057-4-3122660905

## 1. Correlation and Causality

By applying the MCA on the truncated matrices  $\hat{X}$  and  $\hat{Y}$  we obtain the series  $x_k$  and  $y_k$  (eqn. A1) which capture the covariance between two variables within a determined  $MCS_k$  (Figure 3). These series derived from each MCA are used to estimate the correlation,  $\rho_i$ , as:

$$\rho(x, y) = \frac{1}{N-1} \sum_{i=1}^N \left( \frac{x_i - \mu_x}{\sigma_x} \right) \left( \frac{y_i - \mu_y}{\sigma_y} \right) \quad (S1)$$

For our purposes, we performed the analysis by lagging both series from 1 to 9 months, and defined a measure of feedback through the ratio between correlations for each lag of each covariance matrix between pairs of variables.

Nevertheless, correlation analyses just quantify the degree of linear association between variables. We overcame such limitation by using causality analyses to quantify the connectivity between variables. Such causality or information transfer has been defined within the framework of information theory [1–4]. Three basic tenets of the information transfer are the following: (1) Causality implies correlation but correlation does not imply causality, (2) Causality implies directionality, which means that the transfer of information detects the direction of information transfer between two systems, and (3) Asymmetry is a basic property of information transfer.

We consider a feedback as a bi-directional causality between two variables. To estimate the information flow, [1] proposes a system of two stochastic differential equations:

$$\frac{\partial x_k}{\partial t} = F_x(x, y, t) + b_{xx}\omega_x + b_{xy}\omega_y \quad (S2)$$

$$\frac{\partial y_k}{\partial t} = F_y(x, y, t) + b_{yx}\omega_x + b_{yy}\omega_y \quad (S3)$$

where  $\omega_x$  and  $\omega_y$  represent white noise; while  $b_{xy}$  and  $F_{x,y}$  are arbitrary functions of  $X$ ,  $Y$  and  $t$ . Liang (2014) proved that it is possible to measure the causality between two series  $X$  and  $Y$  through the absolute rate of information flow ( $T_{Y \rightarrow X}$ ) in terms of the Shannon entropy, such that:

$$T_{Y \rightarrow X} = -E \left( \frac{1}{\delta_x} \frac{\partial(F_x \delta_x)}{\partial x} \right) + \frac{1}{2} E \left( \frac{1}{\delta_x} \frac{\partial^2 (b_{xx}^2 + b_{xy}^2) \delta_x}{\partial x} \right) \quad (S4)$$

where  $\delta_x$  is the marginal density of  $x$ , and  $E$  represents the expected value [1]. By applying eqn. (S4) to two series  $X$  and  $Y$ , the maximum likelihood estimator of eqn. (S4) is given by,

$$T_{y \rightarrow x} = \frac{C_{xx}C_{xy}C_{y,dx} - C_{xy}^2C_{x,dy}}{C_{xx}^2C_{yy} - C_{xx}C_{xy}^2} \tag{S5}$$

where  $C_{xx}$ ,  $C_{xy}$ ,  $C_{yy}$ ,  $C_{y,dx}$  and  $C_{x,dy}$  denote the possible covariance between series. To estimate  $C_{x,dy}$  and  $C_{y,dx}$  it is necessary to estimate the covariance between pairs of series  $(x, y_n)$  and  $(y, x_n)$ , where  $x_n$  and  $y_n$  are the discrete approximations of  $\frac{dx}{dt}$  and  $\frac{dy}{dt}$ , through the Eulerian formulation:

$$\dot{x}_n = \frac{x_{n+\kappa} - x_n}{\kappa \Delta t} \tag{S6}$$

with  $\kappa=1$ . In some cases, such as deterministic chaotic processes,  $\kappa = 2$ .

The rate of information flow ( $T_{y \rightarrow x}$ ) can be zero or different than zero. If  $T_{y \rightarrow x} = 0$  then  $y$  does not cause  $x$ . There are two possible ways to interpret the information flow depending on the sign: a positive sign of  $T_{y \rightarrow x}$  implies that  $y$  acts upon  $x$  by augmenting its uncertainty, while a negative sign indicates that  $y$  stabilizes  $x$  by diminishing its entropy. This type of interpretation is rather confusing because it goes against the ordinary algebraic interpretation. Diverse similar metrics do exist within the context of information theory, such as the Interaction Information, whose positive (negative) values determine redundancy (synergy) in the interaction between two series [5,6].

Derivation of eqn. (S4) uses the concept of Shannon or Absolute Entropy [7]. For two-variable systems, Liang (2013) proved that the flow of information,  $T_{y \rightarrow x}$ , is the same for both absolute and relative entropy. The latter is more suitable to study predictability, owing to its invariance properties under non-linear interactions [2,5,7].

A measure of relative flow of information [4], in terms of the marginal entropy, can be given as,

$$Z_{y \rightarrow x} = |T_{y \rightarrow x}| + \left| \frac{dH_y}{dt} \right| + \left| \frac{dH_y^{noise}}{dt} \right| \tag{S7}$$

The maximum likelihood estimators suitable to solve eqn.(S7), are:

$$p = \frac{C_{yy}C_{x,dx} - C_{xy}C_{y,dx}}{\det(C)} \tag{S8}$$

$$q = \frac{C_{yy}C_{x,dx} - C_{xy}C_{y,dx}}{\det(C)} \tag{S9}$$

Additionally, the two components of entropy (eqn. A7), estimated in terms of  $p$  and  $q$  are [3]

$$\left| \frac{dH_y^*}{dt} \right| = p \tag{S10}$$

$$\left| \frac{dH_y^{noise}}{dt} \right| = \frac{\Delta t}{2C_{xx}} (C_{dx,dx} + p^2C_{xx} + q^2C_{yy} - 2pC_{dx,x} - 2qC_{dx,y} + 2pqC_{xy}) \tag{S11}$$

Finally, the Relative Flow of Information ( $\tau_{y \rightarrow x}$ ) is defined as:

$$\tau_{y \rightarrow x} = \frac{Z_{y \rightarrow x}}{T_{y \rightarrow x}} \tag{S12}$$

If  $\tau_{y \rightarrow x} = 100$ , the variation of  $x$  is 100% due to the flow of information from  $y$ ; and if  $\tau_{x \rightarrow y} = 0$ , then  $y$  is not the cause. Nevertheless,  $\tau_{y \rightarrow x}$  evaluates the degree influence of  $y$  on  $x$  relative to other processes.

## 2. Appendix B Connectivity of Graphs at Interannual Time Scale

We use graphs to infer structural relations and cycles in the LAFs over TropSA [5]. To that end, graphs must be represented through matrices. There is a mathematical connection between graphs

and the algebraic properties of such matrices [6,8–10]. From this point of view, a graph,  $\Gamma_k$ , has two important matrices associated: the adjacency matrix ( $W$ ) and the Laplacian matrix ( $L$ ).

The adjacency matrix,  $W_{[ixj]}$  (Equation S13), is a square matrix whose dimensions, rows ( $i$ ) and columns ( $j$ ), represent the nodes of a graph. A null entry in this matrix indicates that there is no edge between nodes  $i$  and  $j$ , and thus:

$$W_{ij} = \begin{cases} w_{ij} : \text{weight in the edge } (i, j) \\ \mathbf{0} : \text{there is no edge between } i \text{ and } j \end{cases} \quad (\text{S13})$$

where  $w_{ij}$  is the correlation,  $\rho(x, y)$ , and/or the relative causality,  $\tau_{x \rightarrow y}$ , between the time series  $x_k$  and  $y_k$  of each  $MCS_k$ . If the graph is unidirectional, the adjacency matrix,  $W \in \mathfrak{R}^{ixj}$  is a symmetric matrix of  $|N_k| \times |N_k|$ , with  $|N_k|$  being the number of variables under analysis.

Figure A1 basically represents a directed graph connecting three nodes  $x_k$ ,  $y_k$  and  $z_k$  using linear ( $\rho$ ) and non-linear ( $\tau$ ) coupling metrics. Particularly, this directed graph is an extension of the two nodes scheme presented in Figure A1 (Right). Each directed graph associates its respective adjacency matrix  $W_{[ixj]}^\rho$  (correlations) and  $W_{[ixj]}^\tau$  (causalities). In each adjacency matrix, we head rows and columns with the variable associated to each node ( $X, Y, Z$ ), and thus we emphasize how this matrix establishes all possible connections between these three nodes.

For example, for the case of the correlation-based graph (Figure A1-Left), the edge  $\rho(x_k, y_k)$  connects the nodes in the X-to-Y direction, while the edge  $\rho(y_k, x_k)$  connects the nodes in the Y-to-X direction. Likewise, in the case of non-linear coupling graphs, the edge  $\tau_{x \rightarrow y}$  connects the nodes in the X-to-Y direction, while the edge  $\tau_{y \rightarrow x}$  connects the nodes in the Y-to-X direction (Figure A1-Right). If this method is applied to the interactions between the  $X$  and  $Z$  nodes and between the  $Y$  and  $Z$  nodes of this graph, we find 6 possible interactions between the three nodes. The diagonal of the adjacency matrix is null because we are not analyzing auto-correlations or auto-causalities.

To study graph properties [11], we initially use the spectral graph theory by applying a Singular Value Decomposition on the adjacency matrix  $W_{[ixj]}$  (Equation S14):

$$W_{[ixj]} = U_{[ixi]} \Sigma_{[ixj]} V_{[jxj]}^T = \sum_{h=1}^i u_h \sigma_h v_h^T = u_1 \sigma_1 v_1^T + u_2 \sigma_2 v_2^T + \dots + u_i \sigma_i v_i^T \quad (\text{S14})$$

This SVD of  $W_{[ixj]}$  provides important information about the structural relations and cycles among variables of the LAF graphs. As the structure of  $W_{[ixj]}$  is designed as to evaluate all the possible interactions among variables, the singular values of eqn. (S14) represent the amount of variance explained by each interaction mode. Also, the largest entries of the main singular vectors  $u_1$  and  $v_1$  of eqn. S14 define the most important variables of each mode of interaction [11].

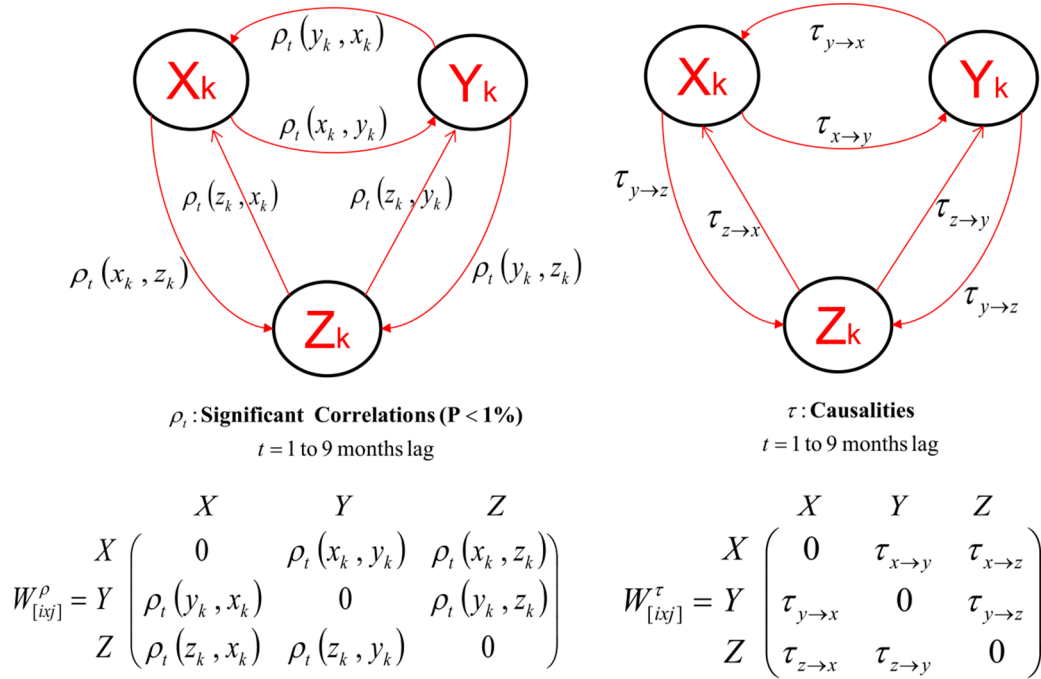


**Figure A1.** Graphs among three variables (X, Y, Z) with links denoting lagged correlations (top left) and causalities (top right) between variables/nodes. Bottom panels include the structure of the graph’s adjacency matrix,  $W$ , to illustrate the node-to-node connection that is established in each graph.

Furthermore, a diagonal matrix of degree  $D \in \mathfrak{R}^{ixj}$  is defined, which quantifies the number of edges per variable; that is the number and cumulative weight of the connections of each node, as

$$D_i = \sum_{\{j|(i,j) \in N_k\}} w_{ij} \tag{S15}$$

From Equations S14 and S15 the Laplacian or Kirchhoff matrix of the graph,  $L \in \mathfrak{R}^{ixj}$ , is estimated as the difference between the degree matrix and the adjacency matrix,  $W_{[ixj]}$ . This implies that the sum of all columns of the Laplacian matrix,  $L(\Gamma_k)$ , adds to zero, so that:

$$L = D - W \tag{S16}$$

$$L_{ij} = \begin{cases} d, & \text{if } i = j \\ -w_{ij}, & \text{if } (i, j) \\ 0, & \text{if there is no edge between } i, j \end{cases} \tag{S17}$$

In this case, we use the spectral graph theory by using eigen-decomposition on the Laplacian matrix to estimate the eigen-values ( $\lambda$ ). These eigen-values contain measures of the connectivity of each graph  $\Gamma_k$  constructed to assess LAFs over TropSA.

Given a graph,  $\Gamma_k$ , and its Laplacian matrix,  $L(\Gamma_k)$ , the eigen-values and eigen-vectors are estimated from

$$L = V\Lambda V^{-1}, \tag{S18}$$

where  $\Lambda = \{\lambda_0, \lambda_1, \lambda_2, \dots, \lambda_i\}$  is a diagonal matrix containing the spectrum of eigen-values of the Laplacian matrix, and the matrix  $V = \{v_0, v_1, v_2, \dots, v_i\}$  contains the eigen-vectors.

The second non-null eigenvalue ( $\lambda_2$ ) of the Laplacian matrix is the algebraic connectivity of the associated graph. This metric was introduced by [9], also known as the Friedler Value. The larger the value of  $\lambda_2$  the larger is the connectivity of  $\Gamma_k$ . Besides, smaller values of  $\lambda_2$  indicates that  $\Gamma_k$  increases its modularity.

Also, the eigen-vector associated with the algebraic connectivity ( $\lambda_2$ ) is known as the Friedler vector ( $v_2$ ). The sign of this eigen-vector can establish a thick partition in two groups of the connected variables of the graph,  $\Gamma_k$ .

Likewise, [10] indicate the following important characteristics of the Laplacian matrix  $L(\Gamma_k)$ :

1.  $L(\Gamma_k)$  is symmetrical,
2. The set of eigen-values and eigen-vectors of  $L(\Gamma_k)$  are real and non-negative,
3. Because of the special structure of the matrix  $L(\Gamma_k)$ , where all entries in each column add up to zero, the smallest eigen-value of this matrix is always zero  $\lambda_0 = 0$  [10].
4. The graph  $\Gamma_k$  has  $h$  connected components if and only if  $\lambda_0 \leq \lambda_1 \leq \lambda_2 \leq \dots \leq \lambda_{h-1} = 0$  [9]. This means that the multiplicity of the null eigen-values ( $\lambda = 0$ ) is the number of components in which the graph  $\Gamma_k$  can be decomposed. The number of null eigen-values corresponds to the number of groups in which the graph can be decomposed.

## References

1. Liang, X.S. Unraveling the cause-effect relation between time series. *Phys. Rev. E* **2014**, *90*, 052150.
2. Schreiber, T. Measuring information transfer. *Phys. Rev. Lett.* **2000**, *85*, 461.
3. Liang, X.S. The Liang-Kleeman information flow: Theory and applications. *Entropy*, **2013**, *15*, 327–360.
4. Liang, X.S. Normalizing the causality between time series. *Phys. Rev. E* **2015**, *92*, 022126.
5. Runge, J. Quantifying information transfer and mediation along causal pathways in complex systems. *Phys. Rev. E* **2015**, *92*, 062829.
6. Kretschmer, M.; Coumou, D.; Donges, J.F.; Runge, J. Using causal effect networks to analyze different Arctic drivers of midlatitude winter circulation. *J. Clim.* **2016**, *29*, 4069–4081.
7. Shannon, Claude E.A Mathematical Theory of Communication. *Bell Syst. Tech. J.* **1948**, *27*, 623–656, doi:10.1002/j.1538-7305.1948.tb00917.x.
8. Donges, J.F., Petrova, I.; Loew, A.; Marwan, N.; Kurths, J. How complex climate networks complement eigen-techniques for the statistical analysis of climatological data. *Clim. Dyn.* **2015**, *45*, 2407–2424.
9. Friedler, M. Algebraic connectivity of graphs. *Czech. Math. J.* **1973**, *23*, 298–305.
10. Pothen, A.; Simon, H.D.; Liou, K.P. Partitioning sparse matrices with eigenvectors of graphs. *SIAM J. Matrix Anal. Appl.* **1990**, *11*, 430–452.
11. Kleinberg, J.M. Authoritative sources in a hyperlinked environment. *J. ACM* **1999**, *46*, 604–632.



© 2018 by the authors; licensee MDPI, Basel, Switzerland. This article is an open access article distributed under the terms and conditions of the Creative Commons by Attribution (CC-BY) license (<http://creativecommons.org/licenses/by/4.0/>).